ADVANCED OPTICAL MATERIALS
www.advopticalmat.de

Color Enrichment Solids of Spectrally Pure Colloidal Quantum Wells for Wide Color Span in Displays

Talha Erdem, Zeliha Soran-Erdem, Furkan Isik, Farzan Shabani, Ahmet Faruk Yazici, Evren Mutlugün, Nikolai Gaponik, and Hilmi Volkan Demir**

Colloidal quantum wells (CQWs) are excellent candidates for lighting and display applications owing to their narrow emission linewidths (<30 nm). However, realizing their efficient and stable light-emitting solids remains a challenge. To address this problem, stable, efficient solids of CQWs incorporated into crystal matrices are shown. Green-emitting CdSe/CdS core/crown and red-emitting CdSe/CdS core/shell CQWs wrapped into these crystal solids are employed as proof-of-concept demonstrations of light-emitting diode (LED) integration targeting a wide color span in display backlighting. The quantum yield of the green- and red-emitting CQW-containing solids of sucrose reach ≈20% and ≈55%, respectively, while emission linewidths and peak wavelengths remain almost unaltered. Furthermore, sucrose matrix preserves ≈70% and ≈45% of the initial emission intensity of the green- and red-emitting CQWs after >60 h, respectively, which is ≈4× and ≈2× better than the drop-casted CQW films and reference (KCl) host. Color-converting LEDs of these green- and red-emitting CQWs in sucrose possess luminous efficiencies 122 and 189 lm W^{-1}_{elect}, respectively. With the liquid crystal display filters, this becomes 39 and 86 lm W^{-1}_{elect}, respectively, providing with a color gamut 25% broader than the National Television Standards Committee standard. These results prove that CQW solids enable efficient and stable color converters for display and lighting applications.

1. Introduction

Within the last 30 years, the lighting technologies have evolved in parallel with the developments in the semiconductor materials. Over the years, general lighting applications witnessed transition from the incandescent lamps to fluorescent lamps and then finally to light-emitting diodes (LEDs).[1] On the other hand, display technologies employed first cathode ray tubes, then fluorescent lamps and more recently LEDs as backlight sources in liquid crystal displays (LCDs). Nowadays displays of organic LEDs[2,3] are also in use and quantum dot LEDs[4,5] and micro-LEDs[6,7] are currently in development. The driving force behind these changes has been partly improving the energy efficiency of the devices but also improving the colorimetric and photometric performance along with realizing a wide color gamut,[8] which can be realized when the spectrally narrow light sources are utilized.[9]

When it comes to narrow-band light sources, the most obvious candidate is the lasers.[10,11] With their linewidths ≈1 nm, these devices offer extremely wide color gamuts and a significant spectral tuning while creating white light. Nevertheless, achieving high efficiencies covering the visible spectrum is currently a significant challenge for the widespread use of lasers in lighting applications.[12,13] The use of multiple LED chips of different colors also suffers from a similar problem. Realizing efficient LEDs in green and yellow colors to obtain white light is a big obstacle for their utilization in lighting.[14–16] Alternatively, colloidal quantum dots offer a solution to this problem as they possess finely tunable emission spectra.[9,17–19] By employing strategically selected quantum dots emitting in specific colors, white

T. Erdem, Z. Soran-Erdem, A. F. Yazici, E. Mutlugün
Department of Electrical-Electronics Engineering
Department of Engineering Sciences
and Department of Nanotechnology Engineering
Abdullah Gül University
Kayseri 38080, Turkey
E-mail: erdem.talha@agu.edu.tr

F. Isik, F. Shabani, H. V. Demir
Departments of Physics, Electrical-Electronics Engineering
and UNAM-Institute of Materials Science and Nanotechnology
Bilkent University
Ankara 06800, Turkey
E-mail: volkan@bilkent.edu.tr

The ORCID identification number(s) for the author(s) of this article can be found under https://doi.org/10.1002/adom.202200161.

N. Gaponik
Physical Chemistry
Technische Universität Dresden
Zellescher Weg 19, 01069 Dresden, Germany

H. V. Demir
LUMINOUS! Center of Excellence for Semiconductor Lighting and Displays
School of Electrical and Electronic Engineering
School of Mathematical and Physical Sciences
School of Materials Science and Engineering
Nanyang Technological University
Nanyang Avenue, Singapore 639798, Singapore

DOI: 10.1002/adom.202200161

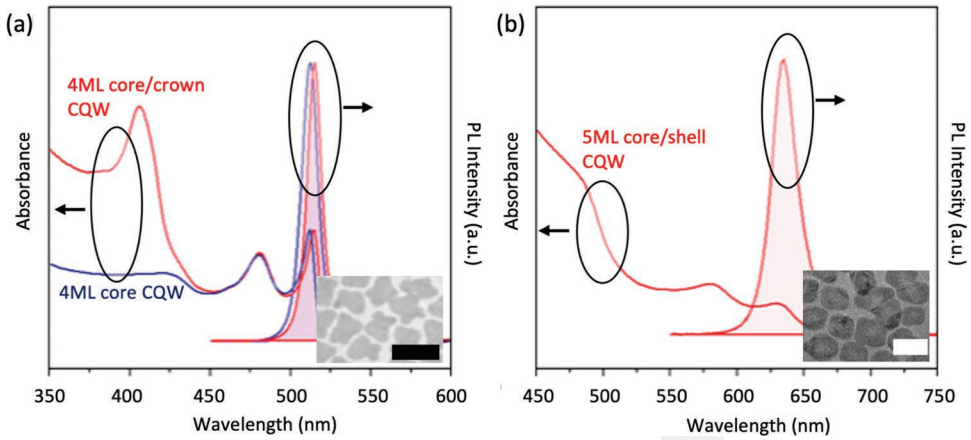

Figure 1. Photoluminescence and absorbance spectra of a) our green-emitting 4 ML CdSe core CQWs (blue), CdSe/CdS core/crown CQWs (red), and b) our red-emitting 5 ML CdSe/CdS core/shell CQWs. Insets: TEM images of the CQWs, scale bar of the 4 ML CQWs: 50 nm, scale bar of the 5 ML CQWs: 20 nm. TEM images of the core CQWs are given in Figure S1 (Supporting Information).

LEDs of quantum dots with high photometric performance have been demonstrated.[18,20,21] Although these nanomaterials exhibit a remarkable level of performance in lighting technologies, achieving a perfect color quality and high photometric efficiency necessitates narrower linewidths than the typical emission linewidths of the quantum dots in solids commonly being >30 nm.

To obtain narrower emission linewidths, a new class of nanomaterials that offer excellent control over the vertical thickness of their quasi-two-dimensional geometry emerged. These atomically flat nanocrystals are known commonly as the colloidal quantum wells (CQWs) or nanoplatelets.[9,22–25] While their lateral dimensions may vary from a few tens of nanometers to one hundred nanometers, their thickness can be precisely controlled in the atomic monolayer level.[22,26] This enables them to emit very pure colors with the emission linewidths ≤30 nm making them excellent candidates for various optoelectronic devices including the lighting applications.[27–29] Nevertheless, ensuring high quantum yields in solid films along with high stability remains a problem.

Embedding these CQWs into crystalline media has the potential to overcome the efficiency and stability issues in solid films.[30,31] Direct incorporation of the CQWs using aqueous salt or sugar solutions requires the CQWs to be transferred into aqueous phase. However, this creates other complications that prevent us from applying these approaches directly to CQWs. For example, when their ligands were changed, we observed that the green-emitting core/crown nanoplatelets stack to each other. As a result, they suffer from a significant reduction in their quantum efficiencies.[32,33] Dispersing the CQWs in tetrahydrofuran and incorporating them into LiCl dissolved in the same solvent[34] also causes a drop in the emission levels of the CQWs, which thus does not allow to make stable solids suitable for use in solid-state lighting and displays.

In this work, to obtain efficient and stable solids of the CQWs, we developed and demonstrated an alternative technique forming solids of sucrose powders specifically enclosing CQWs by quickly evaporating hexane in the mixture of CQWs in vacuum for the first time. To compare with the original method,[35] we also incorporated CQWs into KCl and tested their performance. We observed that the green-emitting core/crown CQWs containing powders of sucrose reach photoluminescence quantum efficiency levels of 19%. Furthermore, incorporating the CQWs into solid pellets protect the emission features of the CQWs. The red-emitting CQWs in sucrose possess a quantum efficiency of 53%. As in the case of green-emitting CQWs, the red-emitting CQWs also preserved their main emission features. Incorporating the CQWs into KCl matrix results in similar quantum efficiencies with incorporating them into sucrose. Nevertheless, the emission stability tests reveal striking differences between these two host media. Encapsulating the green-emitting CQWs within sucrose retains 70% of the initial quantum efficiency after 65 h of exposure to ambient atmosphere whereas the quantum efficiency of the same CQWs in KCl powders and the CQW solid films drop to 35% and 16% of the initial quantum efficiency, respectively. The red-emitting CQWs retained 45% and 24% of the initial intensity when embedded into sucrose and KCl, respectively, whereas the drop-casted red-emitting CQWs retained 22% of the original intensity. These findings indicate that integrating the CQWs in sucrose powders make efficient and stable color converting solids. Moreover, the remarkable spectral purity of the CQWs can be protected in these solids, which makes them highly promising for artificial lighting and displays.

2. Results and Discussion

With the motivation of developing light-emitting devices with extremely pure colors, here we synthesized CQWs possessing very narrow emission linewidths, incorporated them into solid media, and integrated them on blue LEDs to obtain color-converting LEDs of CQWs with high color purity.

We started our experiments by synthesizing two different CQWs that emit in green and red colors. The green-emitting nanoplatelet we synthesized is a four-monolayers-thick CdSe/CdS core/crown CQW. As shown in **Figure 1**, this nanoparticle emits at 510 nm with a full-width at half-maximum of 10 nm. We measured the fluorescence quantum yield of these CQWs as 71%. The red-emitting nanoplatelets we employed in this work were

Table 1. Peak emission wavelengths (λ_{peak}), emission linewidths ($\Delta\lambda_{peak}$), and quantum yields of the green-emitting CQW containing KCl and sucrose pellets. The stock CQW dispersion employed has an optical density of 20 at a wavelength of 400 nm.

Volume of CQW added	λ_{peak} of CQWs in KCl pellets	$\Delta\lambda_{peak}$ of CQWs in KCl pellets	Quantum yield of CQWs in KCl pellets	λ_{peak} of CQWs in sucrose pellets	$\Delta\lambda_{peak}$ of CQWs in sucrose pellets	Quantum yield of CQWs in sucrose pellets
50 µL	517 nm	12 nm	12.3%	519 nm	12 nm	18.3%
100 µL	517 nm	12 nm	18.5%	520 nm	12 nm	15.3%
150 µL	518 nm	13 nm	20.9%	522 nm	12 nm	19.1%

synthesized based on the five-monolayers-thick CdSe core CQWs. When these nanoplatelets were covered with a shell of CdS, the emission of the CQWs red-shifted to 632 nm. The resulting nanoparticles possess a full-width at half-maximum of 25 nm and a quantum yield of 77% (Figure 1). After almost 18 months of their synthesis, the efficiencies of these CQWs in dispersion became 40% and 70%, for the green- and red-emitting CQWs, respectively. These results prove the high stability of the CQW dispersions in hexane, especially that of the red-emitting CQWs.

Using the freshly synthesized green- and red-emitting CQWs, we first incorporated these nanoplatelets into salt (KCl) and sucrose powders as described in the Experimental Section. While preparing the powders, we employed various amounts of CQWs for both types of the nanoparticles (see the Experimental Section). After forming the pellets of these powders, we recorded their emission features including the peak emission wavelength, emission linewidth, and photoluminescence quantum efficiency (**Table 1**).

The peak emission wavelength of the green-emitting CQWs in KCl and sucrose red-shifted compared to their dispersion. The red shift is stronger in the sucrose pellets than the KCl pellets and becomes larger with increasing CQW amount for both KCl and sucrose pellets. We attribute this larger shift in sucrose pellets to the higher refractive index of the host medium ($n_{sucrose}$ = 1.55[36], n_{KCl} = 1.49[37]). The emission linewidths of the CQWs take values between 12 and 13 nm for all the pellet types while the emission linewidths of the dispersion are ≈10 nm. This shows that these pellets successfully preserve the narrow emission bands. The photoluminescence spectra presented in **Figure 2** show a weak broad peak around 700 nm that likely occurs due to the recombination in the deep trap states of the CQWs. The photoluminescence quantum efficiency measurements show that the efficiency of the CQW containing KCl pellets is sensitive to the CQW loading and takes values between 12.3% and 20.9%. On the other hand, the CQW containing sucrose pellets have similar quantum efficiencies (between 15.3% and 19.1%) despite various amounts of CQW loading. These values, however, are much lower compared to the quantum efficiency of the CQW dispersion (71%) showing that the salt or sucrose cannot preserve the initial quantum yields of the green-emitting core-crown CQWs as opposed to the case of QDs.[34] The regions with higher and lower CQW densities on the pellets can be easily spotted by the eye. This means that there is nonradiative energy transfer taking place between the CQWs that are positioned very close to each other on the host powders. This nonradiative energy transfer between the same type of CQWs can partially explain the decreased quantum efficiency. Additionally, samples with KCl may suffer from the halide exchange due to the presence of Cl-ions.[38,39] To study this phenomenon, we compared the photoluminescence lifetimes of the CQWs in sucrose and KCl as 8.3 and 2.4 ns, respectively, for the green-emitting CQWs (Figure S2, Supporting Information). For the red-emitting CQWs, the lifetimes became 19.1 ns for both sucrose and KCl. These results suggest that halide exchange is very likely to have occurred in the green-emitting samples embedded into KCl leading to shorter lifetimes compared to the samples in sucrose due to increased nonradiative recombination rates. For the red-emitting CQWs, similarly recorded lifetimes between the samples with KCl and sucrose indicate that the shell structure seems to protect the CQWs against the halide exchange.

The red-emitting CQWs in pellets have similar optical features to the green-emitting CQWs as summarized in **Table 2**

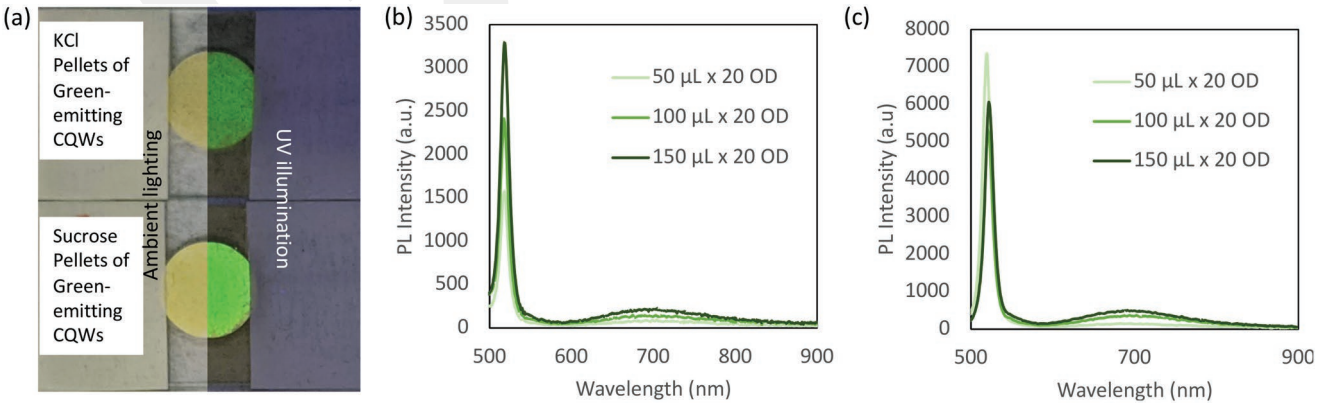

Figure 2. a) Photos of the green-emitting CQW pellets of KCl and sucrose under ambient lighting and UV illumination, b) photoluminescence spectra of the CQW-containing KCl pellets, and c) photoluminescence spectra of the CQW-containing sucrose pellets.

Table 2. Peak emission wavelengths (λ_{peak}), emission linewidths ($\Delta\lambda_{peak}$), and quantum yields of the red-emitting CQW containing KCl and sucrose pellets. The CQW dispersion employed has an optical density of 20 at a wavelength of 400 nm.

Volume of CQW employed	λ_{peak} of CQWs in KCl pellets	$\Delta\lambda_{peak}$ of CQWs in KCl pellets	Quantum yield of CQWs in KCl pellets	λ_{peak} of CQWs in sucrose pellets	$\Delta\lambda_{peak}$ of CQWs in sucrose pellets	Quantum yield of CQWs in sucrose pellets
50 µL	631 nm	23 nm	31.3%	633 nm	25 nm	50.0%
100 µL	633 nm	25 nm	55.0%	635 nm	26 nm	53.0%
150 µL	634 nm	25 nm	54.0%	637 nm	26 nm	45.2%

and **Figure 3**. The red-emitting CQWs experience a red shift when they are incorporated into sucrose and KCl. While the red shift increases with the increasing amount of employed CQWs, the shift is larger in sucrose pellets compared to KCl as in the case of green CQWs. The CQWs in sucrose have a slightly broader emission with the linewidths ≈25–26 nm compared to the KCl pellets possessing linewidths ≈23–25 nm while the emission linewidth of the dispersion is ≈21 nm. The quantum yield of the red-emitting CQWs in KCl pellets is 31% at low nanomaterial concentrations and reaches ≈55% when higher CQW amounts are employed. On the other hand, the sucrose pellets have quantum efficiencies varying between 45% and 53%. These results show that KCl host is a better medium for obtaining a solid with a higher quantum efficiency.

To enable ubiquitous use of CQWs in lighting applications, achieving emission stability is as important as protecting the key emission features and having a high quantum efficiency. For this purpose, we selected the KCl and sucrose pellets containing green- and red-emitting CQWs having the highest quantum yield. We tested the emission spectra and fluorescence lifetime of these pellets together with the drop-casted films of these CQWs as a function of the time when the samples were left in the ambient atmosphere for 65 h.

Results presented in **Figure 4** show that the drop-casted, green-emitting CQWs quickly degraded, and their emission intensity drops to less than 20% of the initial intensity after 65 h. At the end of the test, the intensity of the green-emitting CQWs in KCl dropped to less than 40% of the initial intensity. On the other hand, the same CQWs in sucrose successfully protect ≈70% of the initial intensity. Although the initial efficiency of the KCl pellets is higher, sucrose protects the CQWs better than the KCl. We think that in addition to the humidity and oxygen diffusion, the lower stability in KCl matrix may stem from the diffusion of the ions in the host to the CQWs that degrades the emission of the nanoplatelets.[39]

The red-emitting CQWs also experienced a significant drop in emission intensity when they were left under ambient atmosphere. The CQWs in sucrose preserves more than 40% of the initial quantum efficiency at the end of the test. While the CQWs degraded slower in sucrose, the drop-casted CQW film and the CQWs in KCl host could sustain only ≈20% of the initial emission at the end of the test. These results indicate that incorporating the red-emitting core/shell CQWs are protected best in the sucrose host.

As a proof-of-concept demonstration, we integrated the green-emitting and red-emitting CQW-containing KCl pellets with the highest CQW loadings to a low-power blue LED for the first time in literature. The luminous efficiency of the green- and red-emitting devices become 122 and 189 lm W^{-1}_{elect}, respectively, where W_{elect} stands for the unit of the supplied electrical power. The spectra of these LEDs are presented in **Figure 5**a. Especially for the display applications, the luminous efficiency of the devices after the liquid crystal display (LCD) filters are more important. Our calculations revealed that the LED employing green- and red-emitting CQWs have luminous efficiencies of 39 and 86 lm W^{-1}_{elect} after the LCD filters, respectively. The CIE 1931 (x,y) color coordinates of the resulting LEDs after optical filters used in LCDs become (0.115, 0.718) and (0.707, 0.293) for the green- and red-emitting CQW containing LEDs, respectively. The blue color coordinate of the LED chip after the light transmits from the blue LCD filter becomes

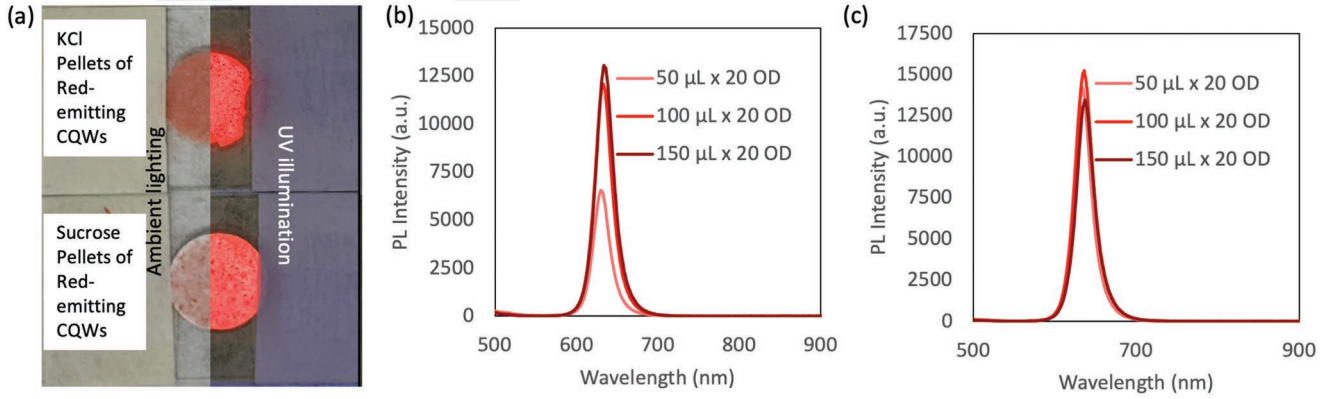

Figure 3. a) Photos of the red-emitting CQW pellets of KCl and sucrose under ambient lighting and UV illumination, b) photoluminescence spectra of the CQW-containing KCl pellets, c) photoluminescence spectra of the CQW-containing sucrose pellets.

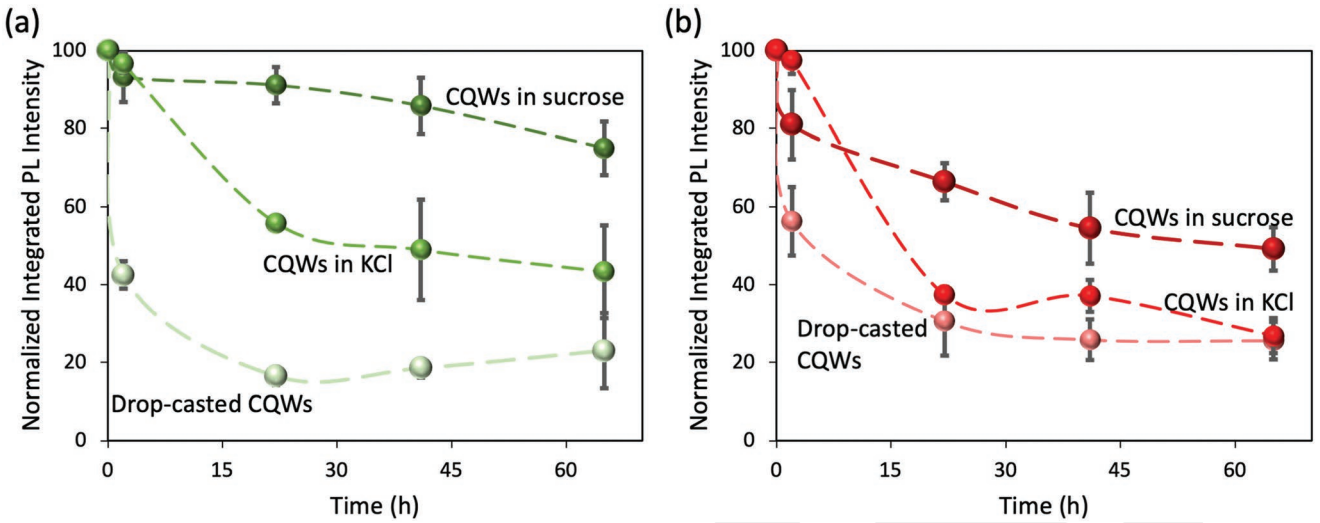

Figure 4. Emission stability of the CQW-containing solids. a) Normalized integrated photoluminescence intensity variation of the drop-casted film of the green-emitting CQWs, green-emitting CQW-containing KCl and sucrose pellets with respect to initial intensity. b) Normalized integrated photoluminescence intensity variation of the drop-casted film of the red-emitting CQWs, red-emitting CQW-containing KCl, and sucrose pellets with respect to initial intensity. The reported values stand for the average of two measurements whereas the error bars denote the standard deviation of these measurements.

(0.154, 0.025). The obtained color gamut presented in Figure 5b suggests a ≈25% broader color gamut than the NTSC standards. These results show that the material system proposed here offers a strong potential in achieving displays possessing a very broad color gamut.

3. Conclusions

In summary, to address the pending challenge of obtaining solids of CQWs while protecting their optical features, in this work, we developed and demonstrated salt and sucrose solids of CQWs, integrated them with an LED for the first time. The green-emitting CQWs embedded into KCl and sucrose achieved a photoluminescence quantum yield of 21% and 19%, respectively, whereas the quantum yield of the CQW dispersion was 71%. The red-emitting CQWs reached quantum yields of 55% and 53% in KCl and sucrose, respectively, while the efficiency of the CQW dispersion was 77%. The photoluminescence peak of these solids red-shifted by a few nm in both media for both types of CQWs compared to the dispersions. The emission linewidths of the green-emitting CQWs remained around 12–13 nm whereas the bandwidth of the red-emitting CQWs became 23–25 nm in KCl host and 25–26 nm in sucrose host.

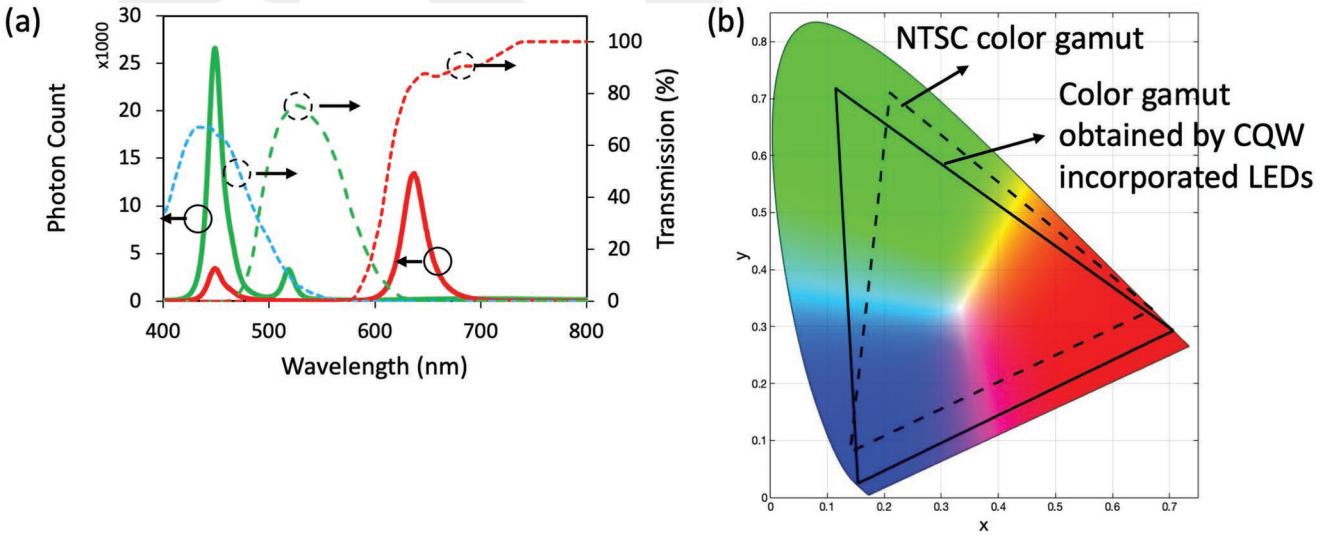

Figure 5. a) Electroluminescence spectra of the LEDs employing green-emitting and red-emitting CQW-containing KCl pellets (continuous lines) along with the LCD filter transmission (dashed lines). b) Color gamut that can be obtained by employing these LEDs in a liquid crystal display (continuous line) compared with the color gamut of the National Television Standards Committee (NTSC) (dashed line).

Compared to the emission linewidths of the dispersions, the linewidths of the pellets broadened only by 2–5 nm, for the green-emitting and red-emitting CQWs. These results show that incorporation into KCl and sucrose successfully protects the narrow-band emission characteristics and peak emission wavelengths of the CQWs. However, the quantum yield of the green-emitting CQWs decreased substantially, showing that additional innovative solutions are necessary to maintain the efficiency of the green-emitting CQWs. We also analyzed the emission stability of these CQW solids by measuring their emission stabilities over time. We found that when left under ambient atmosphere, the green-emitting CQWs in sucrose maintain more than 70% of their initial emission intensity after >60 h while KCl matrix could only maintain less than 40% of the initial emission intensity. Although both host media performed better than the drop-casted film left in the ambient atmosphere that lost more than 80% of the initial intensity, the sucrose matrix is significantly more successful in protecting the green-emitting CQWs. For the red-emitting CQWs, CQWs in KCl did not perform better than their drop-casted film in terms of emission stability while the sucrose matrix preserved more than 45% of the initial emission intensity. These results suggest that although CQWs in KCl matrix achieve a slightly higher quantum yield, the sucrose matrix maintains the emission characteristics of the CQWs making them more suitable for display and lighting applications. As a proof-of-concept device, we demonstrated color-converting LEDs made of green- and red-emitting CQW-containing solids. We showed that using these devices a 25% broader color gamut can be obtained compared to the National Television Standards Committee standards while the luminous efficiency of such green- and red-emitting CQW integrated devices employed together with LCD filters were calculated as 39 and 86 lm W^{-1}_{elect}, respectively. We believe that the outcomes of this work may pave the way for a more wide-spread utilization of CQWs in display and general lighting applications.

4. Experimental Section

Synthesis of CQWs: Syntheses of the green- and red-emitting CQWs were carried out according to refs. [40, 41] and explained in detail in the Supporting Information.

Preparation of Pellets: Embedding the CQWs into sucrose and KCl powders were carried out using ref. [35] and the pellets were prepared according to ref. [42]. Briefly, the sucrose and KCl were powdered using a mortar as finely as possible. Prior to embedding the CQWs into sucrose or KCl powders, the concentration of the green- and red-emitting stock CQW dispersions was set such that the optical density of the 40× diluted dispersions in hexane becomes 0.5 at the wavelength of 400 nm, making the optical density of the stock solution 20. Subsequently, 50, 100, or 150 µL of the CQW stock solution were diluted in 1.5 mL hexane. Next, 250 mg of the finely powdered sucrose or KCl were mixed with the CQW dispersion in a vial and stirred vigorously for 5 min. The samples were then transferred to a desiccator and hexane was evaporated under vacuum for 30 min. After the samples dried, 125 mg of the obtained powders were loaded to a Specac hydraulic press and the pellets were formed by applying a pressure of 10 tonnes cm^{-2} for 10 min. The quantum yield and optical spectroscopy measurements were taken right after the pellets were formed. To obtain the LEDs, the pellets were integrated with a low power blue LED using a two-component epoxy as described in refs. [42, 43].

Optical Characterizations: Photoluminescence spectra of the samples were recorded using a solid sample holder equipped Agilent spectrophotometer. The absorbance spectra of the CQWs were taken using a Thermo Fisher Genesis 10 UV–vis spectrometer. Photoluminescence lifetimes were measured using a PicoQuant Fluotime 100 time-correlated single-photon counting system. The photoluminescence quantum yield of the CQW dispersions was measured using a reference dye (Rhodamine 6G for the green-emitting CQWs and sulforhodamine 101 for red-emitting CQWs). The quantum yield of the pellets was measured using an integrating sphere equipped Hamamatsu C9920 quantum yield measurement system. The photoluminescence stability test was carried out by measuring the spectra of the samples using an Agilent Cary Spectrophotometer at an excitation wavelength of 400 nm having an irradiance of 8.6 µW cm^{-2}.

Supporting Information

Supporting Information is available from the Wiley Online Library or from the author.

Acknowledgements

The authors acknowledge Tübitak-BMBF Bilateral Program Grant Nos. 115F297 and 01DL20002. N.G. and H.V.D. acknowledge long-time cooperation and multiple fruitful discussions with Prof. Jochen Feldmann. H.V.D. gratefully acknowledges support from TÜBA. The authors thank BEU for helpful discussions.

Conflict of Interest

The authors declare no conflict of interest.

Data Availability Statement

The data that support the findings of this study are available from the corresponding author upon reasonable request.

Keywords

colloidal quantum wells, displays, emission stability, lighting, nanoplatelets

Received: January 22, 2022
Revised: April 22, 2022
Published online: June 6, 2022

[1] E. F. Schubert, *Light-Emitting Diodes*, Cambridge University Press, New York, **2006**.
[2] Y. Huang, E. L. Hsiang, M. Y. Deng, S. T. Wu, *Light: Sci. Appl.* **2020**, *9*, 105.
[3] A. Monkman, *ACS Appl. Mater. Interfaces* **2022**, *14*, 20463.
[4] S. Y. Bang, Y. H. Suh, X. B. Fan, D. W. Shin, S. Lee, H. W. Choi, T. H. Lee, J. Yang, S. Zhan, W. Harden-Chaters, C. Samarakoon, L. G. Occhipinti, S. D. Han, S. M. Jung, J. M. Kim, *Nanoscale Horiz.* **2021**, *6*, 68.
[5] Y. M. Huang, K. J. Singh, A. C. Liu, C. C. Lin, Z. Chen, K. Wang, Y. Lin, Z. Liu, T. Wu, H. C. Kuo, *Nanomaterials* **2020**, *10*, 1327.

[6] Y. Wu, J. Ma, P. Su, L. Zhang, B. Xia, *Nanomaterials* **2020**, *10*, 2482.
[7] X. Zhou, P. Tian, C. W. Sher, J. Wu, H. Liu, R. Liu, H. C. Kuo, *Prog. Quantum Electron.* **2020**, *71*, 100263.
[8] T. Erdem, H. V. Demir, *Color Science and Photometry for Lighting with LEDs and Semiconductor Nanocrystals*, Springer, Singapore, **2019**.
[9] T. Erdem, H. V. Demir, *Nanophotonics* **2016**, *5*, 74.
[10] N. Trivellin, M. Yushchenko, M. Buffolo, C. De Santi, M. Meneghini, G. Meneghesso, E. Zanoni, *Materials (Basel)*. **2017**, *10*, 1166.
[11] A. Neumann, J. J. Wierer, W. Davis, Y. Ohno, S. R. J. Brueck, J. Y. Tsao, *Opt. Express* **2011**, *19*, A982.
[12] Q. Zhang, Q. Shang, R. Su, T. T. H. Do, Q. Xiong, *Nano Lett.* **2021**, *21*, 1903.
[13] S. Ji, S. Liu, X. Lin, Y. Song, B. Xiao, Q. Feng, W. Li, H. Xu, Z. Cai, *ACS Photonics* **2021**, *8*, 2311.
[14] S. Pleasants, *Nat. Photonics* **2013**, *7*, 585.
[15] Y. Jiang, Y. Li, Y. Li, Z. Deng, T. Lu, Z. Ma, P. Zuo, L. Dai, L. Wang, H. Jia, W. Wang, J. Zhou, W. Liu, H. Chen, *Sci. Rep.* **2015**, *5*, 10883.
[16] M. Rolles, B. Hyot, P. Miska, *Phys. Status Solidi RRL* **2018**, *12*, 1800173.
[17] T. Erdem, H. V. Demir, *Nanophotonics* **2013**, *2*, 57.
[18] S. Nizamoglu, T. Erdem, X. W. Sun, H. V. Demir, X. Wei Sun, H. Volkan Demir, X. W. Sun, H. V. Demir, *Opt. Lett.* **2010**, *35*, 3372.
[19] T. Erdem, H. V. Demir, *Nat. Photonics* **2011**, *5*, 126.
[20] E. Mutlugun, P. L. Hernandez-Martinez, C. Eroglu, Y. Coskun, T. Erdem, V. K. Sharma, E. Unal, S. K. Panda, S. G. Hickey, N. Gaponik, A. Eychmüller, H. V. Demir, *Nano Lett.* **2012**, *12*, 3986.
[21] T. Erdem, Y. Kelestemur, Z. Soran-Erdem, Y. Ji, H. V. Demir, *Nanophotonics* **2014**, *3*, 373.
[22] A. Riedinger, F. D. Ott, A. Mule, S. Mazzotti, P. N. Knüsel, S. J. P. Kress, F. Prins, S. C. Erwin, D. J. Norris, *Nat. Mater.* **2017**, *16*, 743.
[23] S. Ithurria, G. Bousquet, B. Dubertret, *J. Am. Chem. Soc.* **2011**, *133*, 3070.
[24] B. T. Diroll, *J. Mater. Chem. C* **2020**, *8*, 10628.
[25] M. Nasilowski, B. Mahler, E. Lhuillier, S. Ithurria, B. Dubertret, *Chem. Rev.* **2016**, *116*, 10934.
[26] M. Olutas, B. Guzelturk, Y. Kelestemur, A. Yeltik, S. Delikanli, H. V. Demir, *ACS Nano* **2015**, *9*, 5041.
[27] A. G. Vitukhnovsky, V. S. Lebedev, A. S. Selyukov, A. A. Vashchenko, R. B. Vasiliev, M. S. Sokolikova, *Chem. Phys. Lett.* **2015**, *619*, 185.
[28] O. Erdem, S. Foroutan, N. Gheshlaghi, B. Guzelturk, Y. Altintas, H. V. Demir, *Nano Lett.* **2020**, *20*, 6459.
[29] Z. Wen, Z. Zhou, H. Liu, Z. Wang, X. Li, F. Fang, K. Wang, K. L. Teo, X. W. Sun, *J. Phys. D: Appl. Phys.* **2021**, *54*, 213002.
[30] M. Adam, N. Gaponik, A. Eychmüller, T. Erdem, Z. Soran-Erdem, H. V. Demir, *J. Phys. Chem. Lett.* **2016**, *7*, 4117.
[31] T. Otto, M. Müller, P. Mundra, V. Lesnyak, H. V. Demir, N. Gaponik, A. Eychmüller, *Nano Lett.* **2012**, *12*, 5348.
[32] B. Guzelturk, M. Olutas, S. Delikanli, Y. Kelestemur, O. Erdem, H. V. Demir, *Nanoscale* **2015**, *7*, 2545.
[33] Z. A. Vanorman, A. S. Bieber, S. Wieghold, L. Nienhaus, *Chem. Mater.* **2020**, *32*, 4734.
[34] T. Erdem, Z. Soran-Erdem, V. K. Sharma, Y. Kelestemur, M. Adam, N. Gaponik, H. V. Demir, *Nanoscale* **2015**, *7*, 17611.
[35] A. Benad, C. Guhrenz, C. Bauer, F. Eichler, M. Adam, C. Ziegler, N. Gaponik, A. Eychmüller, *ACS Appl. Mater. Interfaces* **2016**, *8*, 21570.
[36] F. Sanjuan, G. Gaborit, J. L. Coutaz, *J. Infrared, Millimeter, Terahertz Waves* **2021**, *42*, 525.
[37] M. Querry, *Optical Constants of Minerals and Other Materials from the Millimeter to the Ultraviolet*, Report No. ADA192210, U.S. Army Chemical Research, Development & Engineering Center, Aberdeen Proving Ground, MD **1987**.
[38] B. T. Diroll, R. D. Schaller, *Chem. Mater.* **2019**, *31*, 3556.
[39] M. Dufour, J. Qu, C. Greboval, C. Méthivier, E. Lhuillier, S. Ithurria, *ACS Nano* **2019**, *13*, 5326.
[40] M. D. Tessier, P. Spinicelli, D. Dupont, G. Patriarche, S. Ithurria, B. Dubertret, *Nano Lett.* **2014**, *14*, 207.
[41] N. Gheshlaghi, S. Foroutan-Barenji, O. Erdem, Y. Altintas, F. Shabani, M. H. Humayun, H. V. Demir, *Nano Lett.* **2021**, *21*, 4598.
[42] Z. Soran-Erdem, T. Erdem, K. Gungor, J. Pennakalathil, D. Tuncel, H. V. Demir, *ACS Nano* **2016**, *10*, 5333.
[43] T. Erdem, M. Idris, H. V. Demir, D. Tuncel, *Macromol. Mater. Eng.* **2017**, *302*, 1700290.